PERGAMON

Continental Shelf Research 22 (2002) 987–1004

CONTINENTAL SHELF RESEARCH

www.elsevier.com/locate/csr

Sediment transport on the Palos Verdes shelf over seasonal to decadal time scales

Patricia L. Wiberg[a,*], David E. Drake[b,1], Courtney K. Harris[a,2], Marlene Noble[b]

[a] *Department of Environmental Sciences, University of Virginia, Charlottesville, VA 22904, USA*
[b] *US Geological Survey, Coastal and Marine Geology, 345 Middlefield Rd., Menlo Park, CA 94025, USA*

Received 16 June 1999; accepted 12 December 2001

Abstract

We combine direct observations, longer-term wave data, and model calculations to characterize resuspension and transport of fine-grained, effluent-affected sediment on the Palos Verdes shelf. Near-bed waves, currents, and suspended sediment concentrations were monitored during the winter of 1992–93 with a bottom tripod and current-meter mooring at a 63-m-deep site. Wave conditions that winter were moderate ($\sim$2 year recurrence interval), and mean current was alongshelf to the northwest; currents were not significantly correlated with wave conditions. Seven wave events during the winter (December–March) produced near-bed wave orbital velocities at the study site in excess of 14 cm s^{-1}, the observed threshold for significant resuspension. Three of these events occurred during the bottom tripod deployment and are characterized by the highest persistent suspended sediment concentrations in the tripod record. Suspended sediment flux was alongshelf to the northwest for 5 of the 6 wave events for which current data were available; one event occurred during low southeast currents. Measured suspended sediment concentration and grain size generally agree with values that were calculated using a shelf sediment transport model with no adjustment of parameters from values determined for two muddy sites on the northern California shelf. We extend our seasonal observations to a period of almost 2 decades by applying the observed thresholds for wave-driven resuspension to near-bed wave conditions calculated from NDBC Buoy 46025 surface wave data. An average of 10 resuspension events per year, with an average duration of 1.6 days, were identified at a water depth of 60 m; the number of events dropped to 3 per year at 90 m, beyond the shelf break. For the majority of these events, calculated net suspended sediment flux is toward the northwest (alongshelf) at an average rate of 140 kg m^{-1} h^{-1}; about a third of the events have net southeastward flux at an average rate of 30 kg m^{-1} h^{-1}. The calculated thickness of the resuspended surface layer of the bed was less than 1 cm for all events at 60 m.

Keywords: Sediment transport; Continental shelf; Southern California; Sediment resuspension; Effluent-affected sediment

1. Introduction

The dispersal of sediment during resuspension events on the Palos Verdes shelf, southern California, is a potentially important transport pathway for contaminants associated with surface and near-surface (<1 m) sediment deposits (Lee

*Corresponding author.
E-mail address: pw3c@virginia.edu (P.L. Wiberg).
[1] Now at: Drake Marine Consulting, Ben Lomond, CA 95005, USA.
[2] Now at: Virginia Institute of Marine Science, Gloucester Point, VA 23062, USA.

0278-4343/02/$ - see front matter
PII: S0278-4343(01)00116-9

et al., 2002). Although somewhat sheltered by offshore islands, the Palos Verdes shelf experiences wave conditions during storms that are capable of resuspending the effluent-affected, fine-grained sediment present on the sea floor in the middle and outer portions of this narrow shelf (Lee et al., 2002). The frequency of resuspension, and the associated rates and directions of suspended-load transport, are of central importance to the question of dispersal of contaminated sediment on this shelf. Prior to this study, however, the data necessary to characterize resuspension and transport of the effluent-affected sediment were not available.

During the winter of 1992–93, a GEOPROBE bottom tripod was maintained at a 63 m site about 1.5 km northwest of a Whites Point 60 m outfall. Summer and winter measurements of near-surface, mid-depth, and near-bottom currents were made at the same site (Noble et al., 2002). These measurements, together with a detailed analysis of bed sediment properties (Drake et al., 2002), allow us to evaluate the sediment transport conditions at a site within the effluent-affected region of the shelf during the winter, when storm and sediment transport potential is highest.

To enlarge the spatial and temporal scope of our analysis, we use a 17-year record of surface wave spectra from a nearby NOAA wave buoy (NDBC Buoy 46025; National Oceanographic Data Center (NODC), 1998, 2000). The potential for wave-driven resuspension at depths ranging from the shoreward edge of the effluent-affected deposit ($\sim$50 m) to the upper slope is determined from bottom wave orbital velocities calculated from the spectral wave data. Overlap between the buoy and GEOPROBE measurements in the winter of 1992–93 provides a test of the accuracy of bottom wave conditions derived from the buoy data.

We use the nearly two-decades of wave data for the Palos Verdes margin to put the winter of 1992–93 into a longer-term context. When combined with a shelf sediment transport model, we are also able to estimate longer-term average transport frequencies, rates, and directions for the effluent-affected sediment on the Palos Verdes shelf. The results have important implications for the fate of DDT in sediment on the Palos Verdes shelf (Sherwood et al., 2002; Wiberg and Harris, 2002). The initial emplacement of effluent material on the seafloor is addressed by Lee et al. (2002).

2. Site description and methods

The central data collection site for this study, referred to as Site B (Fig. 1), is located at a depth of 63 m on the Palos Verdes shelf (33°42.53′N 118°21.35′W). Site B is near one of the sites (6C) where the Los Angeles County Sanitation District (LACSD) has conducted repeated bed sampling since the1970's (Stull et al., 1986, 1988; Lee et al., 2002).

Wet sieving of the bed surface (0–2 cm) sediment at Site B (Core 147) indicates that it contained 34% sand-sized material, 41% medium-coarse silt and 25% fine silt and clay-sized material (Drake et al., 2002). The density of the sand-sized fractions was significantly lower than the density of quartz, and microscopic analysis of this material revealed that most of these larger particles were fecal pellets (Drake et al., 2002). Comparison of wet-sieved and fully disaggregated samples from Site B (Core 147) suggests that about 40% of the 63–125 μm sediment and >90% of the >125 μm sediment in the upper 2 cm of the bed was pelletized. Average organic content of the bed

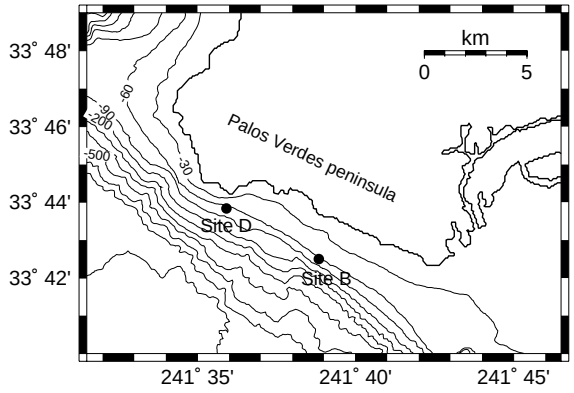

Fig. 1. Location map of the Palos Verdes shelf study area near Los Angeles, California. A GEOPROBE tripod was deployed at Site B and current-meter moorings were deployed at Sites B and D during the winter of 1992–93. NDBC Buoy 46025 is located at 33°44.8′N, 119°4.1′W, about 80 km west of the Palos Verdes shelf (see Fig. 1, Noble et al., 2002).

surface sediment was 3%, with the highest organic fractions in the <20 and $>125\,\mu m$ size classes (Drake et al., 2002; Wiberg and Harris, 2002).

A GEOPROBE bottom tripod (Cacchione and Drake, 1990) was deployed at Site B on 10 December 1992. The tripod was recovered for data retrieval and refurbishment on 14 January 1993 and redeployed on 26 January 1993. It was turned around again between 16 and 18 February 1993 and was recovered on 25 March 1993. We refer to these three deployments as B1, B2, and B3 (Fig. 2). A summary of the positions and sampling schemes for the sensors used in this study are provided in Table 1. Hourly currents, pressure and light attenuation (turbidity) are averages of 17 min time series sampled at a frequency of 1 Hz that were collected once an hour. Hourly near-bed wave orbital velocities, periods and directions were calculated from the 17-min time series of flow velocity after the mean current was removed. We characterize near-bed wave orbital velocity as the "significant" value, u_{bs}, following the convention of characterizing hourly surface wave conditions in terms of significant wave height; u_{bs} was calculated as $\sqrt{2}$ times the rms orbital velocity determined from the velocity variance (Madsen et al., 1993). Wave direction was taken as the direction of the principle component of the velocity variance. Average near-bed wave period, T_{bav}, was calculated from the mean frequency of the velocity variance. Video images of the seabed were made every half hour and the bed was photographed every 4 h.

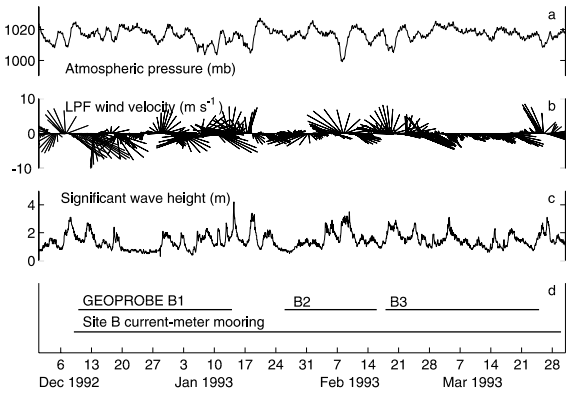

Fig. 2. (a) Atmospheric pressure, (b) low-pass filtered (LPF) wind velocity vectors, and (c) significant wave height during the 1992–93 winter GEOPROBE and mooring deployments at Site B. The deployment periods are indicated in (d). Meteorological and wave data are from NDBC Buoy 46025 (NODC, 1998, 2000).

Near-bed turbidity obscured most of the images of the bed taken by the GEOPROBE. However, several clear images were obtained during low flow conditions in December and February that show the character of the bed. Biogenic tracks and mounds dominated bed roughness in December. The mounds were about 1 cm high and were formed by the accumulation of fecal pellets produced by burrowing organisms. Such pellets were found in bed sediment samples, as noted above. An image from 17 February showed that the effect of a storm was to reconfigure the bed surface into small, low-amplitude, poorly formed ripples whose development was aided by the presence of sand-sized fecal pellets in the surface sediment. The orientation of the ripples indicates that waves were principally responsible for their production.

Six 400–800 ml pump samples of water and suspended sediment were taken simultaneously at two elevations, 0.3 and 1.0 m above bottom (mab), during each GEOPROBE deployment. Preset turbidity thresholds were established to initiate the collection of pumped water samples. Particulate mass for each sample was measured and information on particle compositions and size distributions was obtained by microscopic analysis; 10 of the 36 samples contained iron oxide grains from corrosion of the fittings on the pumping system and are not considered in this analysis.

The correlation is relatively high ($r^2 = 0.80$; Fig. 3b) between light attenuation measured by the GEOPROBE transmissometers and particle concentrations measured from the pump samples. Some of the scatter can be attributed to differences in sampling duration (about 20–40 s for the pump samples vs. 17 min for the light attenuation measurements), differences in sampling time (transmissometer measurements are made prior to pump sampling) and size-dependence in the transmissometer response to sediment in the water column.

To relate transmissometer measurements of light attenuation to suspended sediment concentration,

Table 1
Summary of GEOPROBE sensor positions and sampling rates

Parameter	Sensor type	Sampling times	Elevation above bed[a] (cm)
Currents	Marsh–McBirney electromagnetic current meter (EMCM)	1024 samples at 1 Hz, hourly	22, 55, 92, 125
Pressure	Paroscientific pressure sensor	1024 samples at 1 Hz, hourly	208
Turbidity	Sea-Tech 10 cm LED transmissometer	1024 samples at 1 Hz, hourly	32, 102, 178
Suspended sediment samples	~750 ml water samples pumped into Teflon sample bags	6 samples at 2 levels during each deployment, taken at preset turbidity thresholds	28, 98

[a] Average sensor elevations; during individual deployments, sensor elevations varied by up to 5 cm from these values.

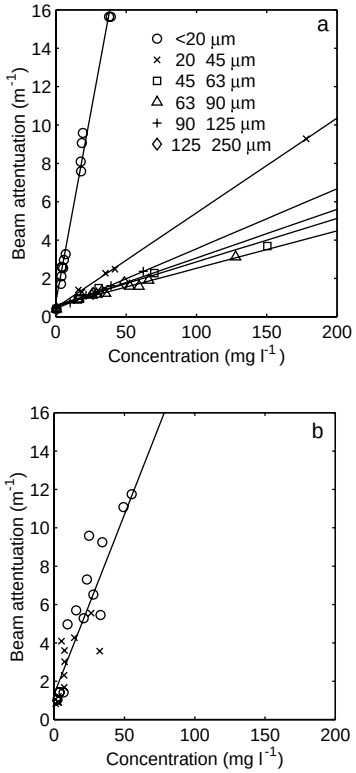

Fig. 3. (a) Size-dependent laboratory calibration of transmissometer measurements of light attenuation against suspended sediment concentration. Lines are best fits to calibration points for each of 6 size fractions as indicated in the legend. (b) Attenuation measured by the 0.3 mab (×) and 1.0 mab (○) GEOPROBE transmissometers against simultaneous pump samples of suspended sediment concentration taken at the same levels during each GEOPROBE deployment. The best-fit line through the data has a slope of 0.22.

a size-dependent calibration was performed in a laboratory calibration tank. Individual calibration curves (Fig. 3a) were measured for each of 6 size fractions obtained from a bed sediment sample from Site B (<20, 20–45, 45–63, 63–90, 90–125 and 125–250 μm).

A current-meter mooring was deployed at Site B for 4 months during the summer of 1992 (21 May 1992–30 September 1992) and 4 months during the winter of 1992–93 (10 December 1992–30 March 1993) (Noble et al., 2002). Hourly average currents, temperature and light transmission (turbidity) were measured 5 and 31 m below the surface and 6 mab using a vector-averaging current meter with attached transmissometer and temperature sensor. A second mooring deployed at Site D (65 m water depth; Fig. 1), northwest of Site B, measured currents 6 mab during the same 4-month winter period and the latter half of the summer period. During the gap between summer and winter mooring deployments, currents at depths of 52, 102, 152 and 196 m below the water surface were recorded at a 200 m-deep mooring site on the slope (Site C; Fig. 1 of Noble et al., 2002). Subtidal currents were obtained by low-pass filtering (cutoff at 35 h) the hourly average currents.

Hourly measurements from 1982–99 of wave height spectra (NODC, 1998, 2000) from NDBC Buoy 46025 (33°44.8′N, 119°4.1′W; Fig. 1 of Noble et al., 2002), located about 80 km west of the Palos Verdes shelf, were used to calculate near-bed wave orbital velocity, u_{bs}, and average period,

T_{bav}, for times and shelf depths not sampled by the GEOPROBE. Full surface wave spectra were used in these calculations (following Harris and Wiberg, 1997) so as to properly account for the differences in attenuation of short and long period waves as a function of water depth. Near-bed wave conditions were calculated for depths ranging from 50 m (shoreward edge of the fine-grained deposit) to 120 m (upper slope).

Values of u_{bs} calculated from surface wave height spectra and from GEOPROBE velocity measurements at Site B are well correlated (correlation coefficients >0.98 for all 3 deployments) during the period of overlap in the winter of 1992–93. Scatter plots of u_{bs} and of T_{bav} from the GEOPROBE and the buoy (Fig. 4) yield relationships with slopes close to one. GEOPROBE values of near-bed wave conditions, particularly wave period, are much noisier than buoy-derived values during deployments B1 and B2; GEOPROBE data plotted in Fig. 4a and b are smoothed with a 5 h running average filter to reduce the high frequency variations. In contrast, GEOPROBE wave data for deployment B3 (Fig. 4c and d) exhibited almost no noisiness. Root-mean-squared differences between GEOPROBE and buoy-derived values of u_{bs} and T_{bav} are 1 cm/s and 0.7 s, respectively, for all data shown in Figs. 4a and b.

3. Bottom-boundary-layer flow and sediment transport at Site B during 1992–93

Mean bottom-boundary-layer currents on the Palos Verdes shelf during summer and winter were predominantly northwestward (Table 2; Noble

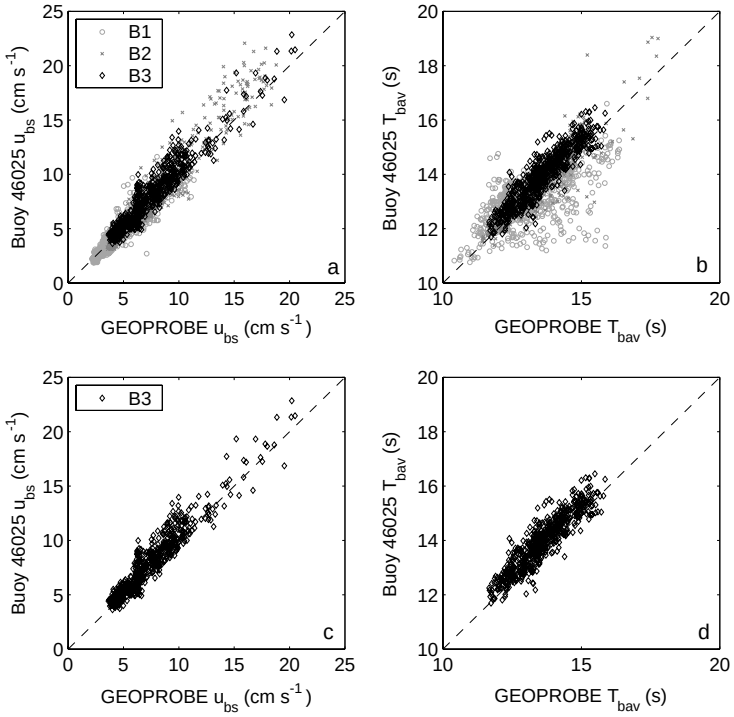

Fig. 4. (a) Scatter plot of near-bed wave orbital velocity determined from GEOPROBE measurements at Site B (depth of 63 m) and from hourly wave height spectral data from NDBC Buoy 46025 during the winter of 1992–93. (b) Hourly average bottom wave period determined from the GEOPROBE data at Site B vs. values determined from Buoy 46025 spectral wave data. (c) Same as (a), but limited to the time of deployment B3 (Fig. 2d) when GEOPROBE values of near-bed wave conditions are least noisy. (d) Same as (b), but limited to the time of deployment B3. The GEOPROBE data in (a)–(d) were smoothed with a 5-h running average filter to reduce high frequency variations present in the T_{bav} and, to a lesser extent, in the u_{bs} time series.

Table 2
Summary of bottom-boundary-layer currents along the 60 m isobath in 1992–93

Site/system	Duration	Height above bed (m)	Alongshelf[a] mean velocity ($cm\,s^{-1}$)	Across-shelf[b] mean velocity ($cm\,s^{-1}$)	Mean current speed ($cm\,s^{-1}$)
Site B					
Mooring	5/21/92–9/12/92	6	1.9	−0.3	7.9
Mooring	12/10/92–3/30/93	6	3.2	−0.0	9.8
GEOPROBE	12/10/92–3/24/93[c]	1.3	2.3	−1.4	8.4
Site D					
Mooring	7/11/92–9/25/92	6	4.2	0.4	9.6
Mooring	12/9/92–3/30/93	6	4.1	0.2	10.7

[a] Positive and negative alongshelf velocities are poleward and equatorward, respectively.
[b] Positive and negative across-shelf velocities are onshore and offshore, respectively.
[c] There are two gaps in the GEOPROBE record when it was recovered for data retrieval and refurbishment (Fig. 2d).

et al., 2002), following the isobaths (oriented 60° west of north). Mean across-shelf velocity at Site B was small and off-shelf during both current-meter mooring deployments (Table 2). The currents displayed little seasonal structure. Variance in the 6-mab currents was split almost equally between tidal and subtidal frequencies. Alongshelf wind stress accounted for only 10–15% of the variability in the subtidal currents (Noble et al., 2002). Peak subtidal currents of $24\,cm\,s^{-1}$ (6 mab), directed poleward alongshelf, were recorded on 20 February (Fig. 5a). The along-shelf component of subtidal, bottom-boundary-layer currents was relatively coherent along the 60 m isobath; the correlation between alongshelf, subtidal currents measured 6 mab at Sites D and B is 0.73. In contrast, the correlation between across-shelf, subtidal currents at the two sites is 0.10. Mean alongshelf current 6 mab at Site D was larger than at Site B, particularly during the summer deployment (Table 2). Mean across-shelf current 6 mab was weakly onshore at Site D and offshore at Site B (Table 2).

Harmonic analysis of the currents 6 mab indicates that the semidiurnal M2 tidal constituent dominated tidal currents. Major and minor axes of the M2 tidal ellipse during the winter deployments were 5.3 and $-0.5\,cm\,s^{-1}$, respectively, with an orientation of 62° west of north (in the alongshelf direction); similar values were observed 6 mab at Site D. The major axis of the M2 tide during the summer deployment at Site B was about $1\,cm\,s^{-1}$ smaller and the orientation was rotated to 10° west of north.

Alongshelf winter currents measured 1.3 mab by the GEOPROBE tripod were poleward, in agreement with the current-meter mooring measurements 6 mab (Table 2). While mean current speed 1.3 mab was 15% smaller than at 6 mab, the across-shelf component of velocity was larger owing to near-bed turning in the bottom boundary layer (Table 2). Alongshelf currents measured by the moored current meter 6 mab and the GEOPROBE current meter 1.3 mab were highly correlated (0.96, Fig. 5a and b); the correlation was somewhat lower (0.59) between mooring and GEOPROBE across-shelf currents. Current shear velocity can be estimated from the 4-point, near-bed current profile measured by the GEOPROBE (e.g., Drake and Cacchione, 1992). The mean value of current shear velocity for the 3 deployments was $0.64\,cm\,s^{-1}$ (standard deviation of $0.28\,cm\,s^{-1}$). Peak current shear velocity was $1.7\,cm\,s^{-1}$.

Average significant wave height recorded by Buoy 46025 from December 1992 through March 1993 (the period spanning the winter tripod and current-meter mooring deployments; Fig. 2) was 1.4 m. A maximum wave height of 4.2 m was recorded on 14 January, just after the end of deployment B1 (Fig. 2). Following this are 3 other wave events with peak significant wave heights in excess of 3 m, one of which occurred during deployment B2 (8–10 February) and one during B3 (4 March; Fig. 2, Table 3). These two events

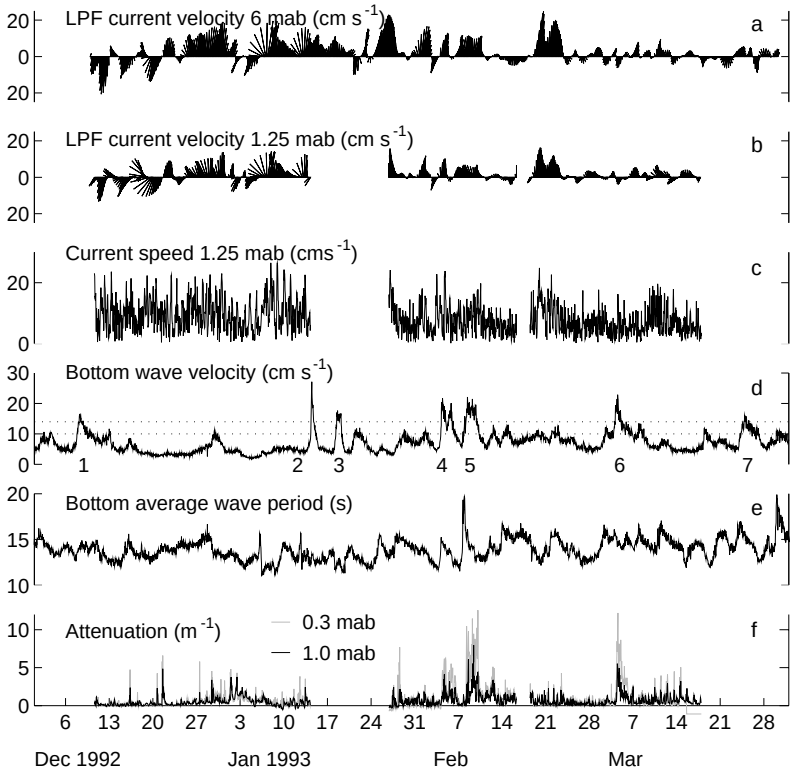

Fig. 5. Data from the (a) winter current-meter mooring and (b, c, f) GEOPROBE deployments at Site B. Currents in (a) and (b) were low-pass filtered (LPF) to remove tidal currents. Wave conditions (d, e) were determined from NDBC Buoy 46025 spectral wave data. The dotted lines in (d) indicate threshold values for non-transport ($u_{bs} \leqslant 10\,\mathrm{cm\,s^{-1}}$) and transport events ($u_{bs} \geqslant 14\,\mathrm{cm\,s^{-1}}$) due to wave-induced bed shear stresses. The 7 wave-driven transport events identified in the wave record at 60 m are numbered in (d).

Table 3
Characteristics of sediment transport events at Site B during winter 1992–93

Event	1	2	3	4	5	6	7
Date	12/8/92	1/14/93	1/18/93	2/4/93	2/7/93	3/4/93	3/24/93
Duration (h)	31	20	22	52	58	45	44
Significant wave height (m)[a]	*2.6*	*2.9*	*3.0*	*2.3*	*2.8*	*2.2*	*1.9*
	3.1	**4.2**	**3.4**	**2.9**	**3.5**	**3.1**	**2.7**
Near-bed wave orbital velocity[a] ($\mathrm{cm\,s^{-1}}$)	*13.4*	*16.0*	*15.0*	*15.3*	*16.4*	*15.0*	*12.8*
	16.5	**27.1**	**17.7**	**21.7**	**22.1**	**22.9**	**16.0**
Alongshelf velocity 6 mab ($\mathrm{cm\,s^{-1}}$)[b]	N/A	*10.3*	*9.0*	*5.2*	*10.2*	*−1.7*	*4.0*
Across-shelf velocity 6 mab ($\mathrm{cm\,s^{-1}}$)[b]	N/A	*1.8*	*0.2*	*0.8*	*0.7*	*−0.2*	*1.1*
Attenuation 0.3 mab[c] ($\mathrm{m^{-1}}$)	N/A	N/A	N/A	*3.0*	*5.8*	*4.4*	N/A
		2.9	3.0	2.9	4.0	3.3	1.5
Attenuation 1.0 mab[c] ($\mathrm{m^{-1}}$)	N/A	N/A	N/A	*1.4*	*2.2*	*1.8*	N/A
		2.1	2.0	2.0	2.7	1.9	1.1
Resuspension depth[d] (cm)		0.11	0.11	0.15	0.11	0.11	0.05
Net suspended sediment flux[d] ($\mathrm{kg\,m^{-1}\,h^{-1}}$)		145	137	90	176	30	34

[a] Italic and bold numbers correspond to mean and maximum values, respectively.
[b] Positive values of alongshelf and across-shelf velocity are poleward and shoreward, respectively.
[c] Italic and underlined numbers correspond to mean measured and calculated values, respectively.
[d] Calculated values.

coincided with the maximum values of light attenuation ($>10\,m^{-1}$, 0.3 mab; Fig. 5f) and near-bed wave orbital velocity ($>20\,cm\,s^{-1}$; Fig. 5d) recorded by the GEOPROBE. One additional wave event (4–6 February) during the period of GEOPROBE deployments produced near-bed wave orbital velocities exceeding $20\,cm\,s^{-1}$; peak significant wave height during this event was 2.9 m (Fig. 2c) and light attenuation 0.3 mab reached $7\,m^{-1}$ (Fig. 5f). Mean near-bed average wave period (T_{bav}) in the GEOPROBE record was 13 s, with a peak value of almost 20 s during the 8–10 February wave event (Fig. 5e). Average direction of wave approach based on the GEOPROBE measurements was 8° south of west; during 84% of the record, waves approached from between 10° north and 30° south of west.

The correlation between near-bed wave orbital velocity and current velocity was insignificant during the period of the current-meter mooring deployments (summer 1992 and winter 1992–93) at Site B. Fifty-six percent of the time when $u_{bs} > 12\,cm\,s^{-1}$, current speed 6 mab was less than $10\,cm\,s^{-1}$. Furthermore, the only time when current speed exceeded $30\,cm\,s^{-1}$ were accompanied by $u_{bs} \leqslant 12\,cm\,s^{-1}$. The lack of correlation between waves and currents suggests that they were independently driven (Noble et al., 2002).

The influence of both tides and wave conditions are apparent in hourly values of light attenuation measured 0.3 and 1.0 mab. Tidal variations in current speed are largely responsible for the higher frequency variations in attenuation observed throughout the record. Values of attenuation that exceeded $4.0\,m^{-1}$ at a height of 1 mab were associated with periods of high waves except for one brief period during the first (B1) deployment. Mean light attenuation was $0.6\,m^{-1}$ at a height of 0.3 mab and $0.5\,m^{-1}$ at 1.0 mab when $u_{bs} \leqslant 10\,cm\,s^{-1}$. In contrast, mean light attenuation was $5.6\,m^{-1}$ (0.3 mab) and $2.3\,m^{-1}$ (1.0 mab) when $u_{bs} \geqslant 14\,cm\,s^{-1}$.

Near-bed wave orbital velocity thresholds of 14 and $10\,cm\,s^{-1}$ are the closest pair of values for defining periods with and without resuspension, respectively, based on a criterion of a factor of 10 change in observed light attenuation 0.3 mab. The lack of a distinct attenuation response in late February and in March when u_{bs} reaches values between 10 and $13\,cm\,s^{-1}$ also suggests that peak u_{bs} values of roughly $14\,cm\,s^{-1}$ or higher are required to produce significant resuspension. Similar near-bed wave orbital velocity thresholds for resuspension were identified at the STRESS mid-shelf site on the Russian River shelf in northern California (Harris and Wiberg, 1997) and at shelf sites off central California (Drake and Cacchione, 1992).

The strong association between high near-bed wave orbital velocities and high turbidity levels is indicative of resuspension of bed sediment during periods of high bed shear stress produced by large surface waves. Near-bed wave orbital velocities of 10 and $14\,cm\,s^{-1}$ correspond to bed shear stresses (skin friction) of roughly 0.8 and $1.4\,dyn\,cm^{-2}$, respectively (Wiberg, 1995). The average, combined wave-current bed shear stress when $u_{bs} = 10\,cm\,s^{-1}$ and $14\,cm\,s^{-1}$ (mean current shear velocity of $0.4\,cm\,s^{-1}$), is $0.9\,dyn\,cm^{-2}$ and $1.6\,dyn\,cm^{-2}$, respectively. Mean current speed and current shear velocity during periods of high turbidity were not significantly different than at other times. Mean attenuation 0.3 mab was 2.4 times higher than at 1.0 mab when $u_{bs} \geqslant 14\,cm\,s^{-1}$, whereas the ratio was only 1.2 when $u_{bs} \leqslant 10\,cm\,s^{-1}$. Steep attenuation gradients during high wave conditions are consistent with resuspension of coarser sediment and increasingly large differences between the shear velocity within the wave boundary layer and above it.

Pump samples of suspended sediment were collected during the resuspension events in early February and early March. Peak measured suspended concentrations during the early February event (0800 on 8 February) were $55\,mg\,l^{-1}$ at a height of 0.3 mab and $32\,mg\,l^{-1}$ at a height of 1.0 mab. Peak hourly average attenuation 0.3 mab for this event ($12\,m^{-1}$; Fig. 5f) occurred during the same hour that the pump sample was collected. Measured suspended concentrations during the early March event (1900 on 4 March) were $34\,mg\,l^{-1}$ (0.3 mab) and $26\,mg\,l^{-1}$ (1.0 mab). Hourly attenuation 0.3 mab peaked 5 h prior to the time when the pump sample was collected for this event; peak attenuation was $13\,m^{-1}$ whereas

attenuation at the time of the pump sample was $9\,m^{-1}$.

Microscopic analysis of the size of sediment in the 4 March 1993 pump samples collected 0.3 mab indicates a median size of roughly 20 μm (55% $<20\,\mu m$, 27% 20–63 μm and 17% 63–125 μm) while sediment sampled 1.0 mab at the same time was finer (75% $<20\,\mu m$, 25% 20–63 μm). The median size of the pump sample collected 0.3 mab on 8 February 1993 was also $<20\,\mu m$ (61% $<20\,\mu m$, 34% 20–63 μm, 5% 63–125 μm). The percentage of suspended sand-sized sediment in the lowest meter of the water column was probably higher than these values indicate. Placement of the pump relative to the sampling bags in the GEOPROBE pump sampler caused some breakage of pellets, which comprised a large portion of the sand-sized material in the seabed. Nevertheless, applying the calibration between concentration and attenuation as a function of grain size (Fig. 3a) to each size fraction in the pump samples, and summing over all fractions (see, e.g., Wiberg et al., 1994), yields estimated attenuations of 14 and $8\,m^{-1}$ at a height of 3 mab for the February and March pump samples, respectively, in good agreement with the measured values.

Pump samples were divided into two groups, predominantly "biogenic" or predominantly "terrigenous", based on an estimate of the relative amounts of plankton detritus and mineral grains in samples filtered through a 47 nm membrane filter. In general, samples with higher (>10 mg/l) concentrations of sediment also had higher concentrations of terrigenous mineral grains such as mica and quartz. Mean size of terrigenous samples was 20–30 μm, with 7–32% of the sediment being coarser than 45 μm. A linear relationship between concentration in pump samples and transmissometer measurements of light attenuation (Fig. 3b) has a slope of 0.22. This is consistent with a grain size of about 24 μm based on the transmissometer calibration curves (Fig. 3a), similar to the mean size of the terrigenous pump samples.

Pump samples with low concentrations contained relatively high proportions of biogenic detritus produced by plankton, with sizes limited to $<45\,\mu m$. The low concentration values ($<\sim 10\,mg\,l^{-1}$) plotted in Fig. 3b follow a trend similar to the transmissometer calibration relationship for the $<20\,\mu m$ fraction (slope of 0.40, Fig. 3a). These results suggest that periods of high concentration correspond to times when mineral grains are resuspended from the bed surface, whereas low concentrations of biogenic detritus dominate suspended particulate matter during less energetic conditions.

A sense of the relative contribution of storms to suspended sediment flux can be obtained by estimating the transport rate 1 mab as the product of velocity and suspended sediment concentration measured near 1 mab (see, e.g., Sherwood et al., 1994; Ogston and Sternberg, 1999). Based on an attenuation vs. concentration slope of 0.40 for periods of low concentration ($u_{bs}<10\,cm\,s^{-1}$) and a slope of 0.22 otherwise (see above; Fig. 3b), measured attenuation was converted to concentration. The highest transport rates 1 mab ($>3\,g\,m^{-2}\,s^{-1}$) occurred during the two resuspension events in early February. Net flux during these events was alongshelf to the northwest. The second of these two events (7–9 February) accounted for 50% of the net alongshelf transport 1 mab during the 3 GEOPROBE deployments. The contribution to net flux of the other two resuspension events was smaller, however. Two periods of high, prolonged northwestward subtidal currents (25 December–14 January and 20 February–23 February; Fig. 5) also contributed 15–20% each to net alongshelf flux 1 mab despite the relatively low waves at these times. Bed shear stress estimates never exceeded threshold values from 1–6 January, despite elevated attenuation, suggesting that the fluxes during this time were not due to resuspension.

4. Characteristics of sediment transport events on the Palos Verdes shelf

The observations described above suggest that the highest near-bed suspended-sediment concentrations at depths near 60 m on the Palos Verdes shelf result from resuspension produced by large surface waves. Thus we expect that surface wave conditions are key to identifying

high-concentration resuspension events within the effluent-affected region of the Palos Verdes shelf. The volume of sediment in suspension depends on the combined wave-current bed shear stress, shear velocity in the bottom boundary layer and wave boundary layer, and the characteristics of the bed surface sediment. Suspended sediment transport rates associated with these resuspension events depend on current speed and direction as well as suspended sediment concentration.

The measurements at Site B provide the necessary information to characterize transport events and non-transport intervals during the deployments in the winter of 1992–93. Based on the analysis presented above, we identify transport events as times when near-bed wave orbital velocity, u_{bs}, exceeded $14\,\mathrm{cm\,s^{-1}}$ and non-transport intervals as times when $u_{bs} \leqslant 10\,\mathrm{cm\,s^{-1}}$ (dotted lines in Fig. 5d). Hours when $10 < u_{bs} < 14\,\mathrm{cm\,s^{-1}}$ immediately preceding or following a transport event were incorporated into that event. Other times with intermediate wave orbital velocities were included in the adjoining non-transport intervals. In this manner, transport events were extended to include a significant part of the waxing and waning of resuspension. This is particularly important following a resuspension event when it can take several hours for the sediment suspended in the bottom boundary layer to settle back to the bed.

Seven transport events were identified using these criteria in the 60 m record of bottom wave conditions calculated from NDBC Buoy 46025 during the winter of 1992–93 (December–March; Fig. 5d, Table 3). These include the three transport events discussed earlier as well as one just prior to the first (B1) deployment, two between deployments B1 and B2 and one following deployment B3 (Fig. 2c, Fig. 5d). Average duration of the 7 events was 39 h (1.6 days; Table 3) and the average interval between events was 18 days. Peak significant wave height for these resuspension events averaged 3.3 m and peak near-bed wave orbital velocity averaged $21\,\mathrm{cm\,s^{-1}}$. The net direction of transport depends on the currents. The mean current 6 mab at Site B (Fig. 5a) for all events except the first, which occurred before the winter current-meter mooring record began, was $5.3\,\mathrm{cm\,s^{-1}}$ alongshelf (poleward) and $0.6\,\mathrm{cm\,s^{-1}}$ across-shelf (shoreward) (Table 3). Mean alongshelf advection distance per storm 6 mab was 7.4 km. However, because 6 mab is well above the center of mass of the sediment in suspension, the mean alongshelf displacement distance of the suspended sediment would have been smaller.

To extend our analysis of transport events on the Palos Verdes shelf spatially and temporally, we made use of the longer time series (1982–99) of surface wave-height data from NDBC Buoy 46025 (NODC, 1998, 2000). Near-bed wave orbital velocities were calculated for depths ranging from 50 m, the shoreward edge of the fine-grained deposit, to beyond the shelf break ($\sim$75 m) for the entire 17-year buoy record. Assuming that resuspension thresholds are similar throughout the fine-grained, effluent-affected portion of the Palos Verdes shelf, we characterize wave-driven transport events at a range of depths across the shelf. Further assuming that the resuspension thresholds identified from the GEOPROBE data can be applied to the entire buoy wave record, we can also extend our analysis of transport events on the Palos Verdes shelf to the period from 1982–99. This last assumption is reasonable, as there have been no major changes since 1985 in discharge from the Whites Point outfall pipes, the primary source of sediment to Site B (Sherwood et al., 2002).

Frequency of resuspension varies across the shelf as a result of the decrease in near-bed wave orbital velocity that accompanies an increase in water depth. During the winter of 1992–93 (December–March), the number of resuspension events ranged from 16 at a depth of 50 m to 0 at a depth of 100 m (Fig. 6a). Mean duration of these transport events also decreased from 1.9 days at 50 m to 0.2 days at 90 m. If the record is extended to the 12-month period from May 1992–April 1993, roughly corresponding to the period of the current-meter mooring deployments, the number of events increases to 24 at 50 m and 8 at 60 m; the number of events remains unchanged at depths of 70 and greater. Of the one event at 60 m and 8 events at 50 m that occurred during months other than December–March, 7 took place in April. The non-winter events at 50 m and 60 m lasted half as long, on average, as the winter events as these depths. The portion of the 12-month record during

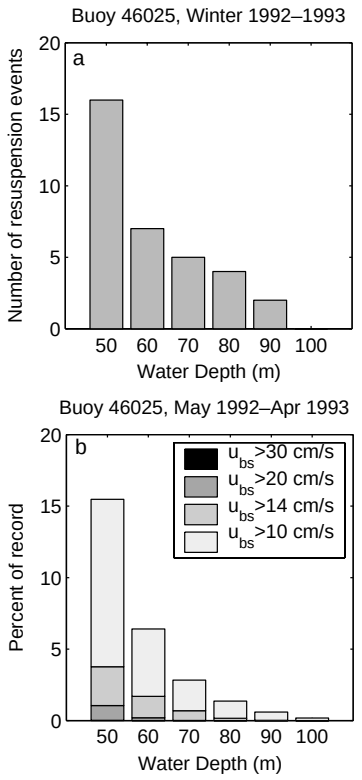

Fig. 6. (a) Number of wave-driven transport events as a function of depth on the Palos Verdes shelf and upper slope during the winter GEOPROBE and current-meter mooring deployments. (b) Percent of time when near-bed wave orbital velocity exceeds the values indicated in the legend during the 12-month period from May 1992–April 1993 for depths ranging from the shoreward edge of the effluent-affected deposit ($\sim$50 m) to the upper slope. Wave conditions are calculated from hourly surface wave spectra measured by NDBC Buoy 46025 (NODC, 1998, 2000). Values of $u_{bs} \geqslant 14\,\mathrm{cm\,s^{-1}}$ are associated with resuspension events.

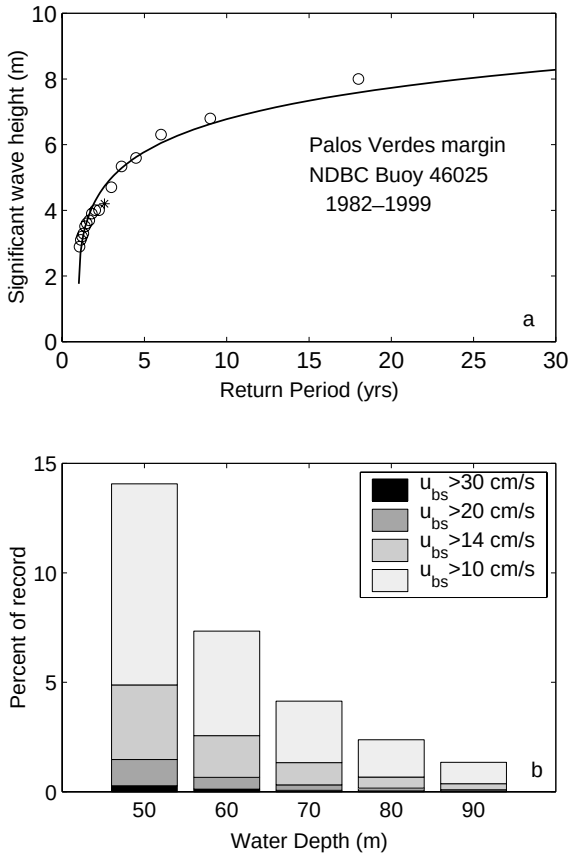

Fig. 7. (a) Recurrence time of annual peak significant wave heights based on the Gumbel distribution applied to the 1982–99 record of surface wave conditions at NDBC Buoy 46025 (NODC, 1998, 2000) on the Palos Verdes margin. Peak significant wave height during the winter of 1992–93 is indicated by an asterisk. (b) Distribution of near-bed wave orbital velocity from the mid-shelf to upper slope during 1982–99.

which $u_{bs} \geqslant 14\,\mathrm{cm\,s^{-1}}$ (Fig. 6b) is therefore dominated by winter storms. This is consistent with the pattern of winter storm-driven transport observed elsewhere on the California shelf (e.g. Drake and Cacchione, 1985, Sherwood et al., 1994; Ogston and Sternberg, 1999).

Sediment transport on the Palos Verdes shelf during the winter of 1992–93 can be put into context by comparing the wave conditions that winter to those in the longer NDBC Buoy 46025 (NODC, 1998, 2000) wave record for the Palos Verdes margin. An analysis of the return period of annual peak wave conditions (Fig. 7a) using a Gumbel distribution (Borgman and Resio, 1982) indicates that the peak significant wave height of 4.2 m reached during the winter of 1992–93 has a return period of 2–3 years. Six of the 17 winters in the buoy record had peak significant wave heights exceeding the 1992–93 value. Maximum recorded wave conditions occurred in January 1988 when significant wave height reached 8 m. Based on the spectral buoy data, waves during January 1988 produced a peak u_{bs} of $63\,\mathrm{cm\,s^{-1}}$ at a depth of 60 m and were sufficient to resuspend sediment at water depths $\leqslant$170 m. The fraction of the year during

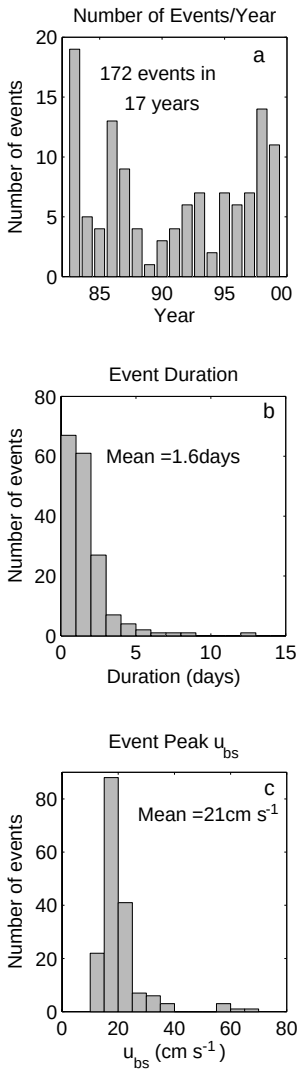

Fig. 8. Characteristics of wave events identified at 60 m for each year of the 1982–1999 NDBC Buoy 46025 record. (a) Number of wave events based on a near-bed wave orbital velocity threshold of 14 cm s^{-1} (see text), (b) distribution of wave event duration and (c) distribution of peak event near-bed wave orbital velocity (u_{bs}) identified in the wave buoy record from 1982–99.

which u_{bs} exceeded 10, 14 and 20 cm s^{-1} in the full 17-year record was similar to 1992–93 (Figs. 6b and 7b). High near-bed wave orbital velocities ($u_{bs} > 30$ cm s^{-1}) were less common than average in 1992–93.

Analysis of wave events in the buoy record indicates considerable year-to-year variability in storminess on the Palos Verdes shelf. At a depth of 60 m, the maximum number of wave events (19) occurred in the winter of 1982–83 (an El Nino year) and the minimum number (1) occurred in the winter of 1988–89 (Fig. 8). An average of 10 wave events occurred each year through the 1980's and 1990's, with no evident trend through those decades in terms of number of events. A total of 172 wave events occurred at a depth of 60 m between October 1982 and October 1999 (17 years), with a mean duration of 1.6 days (Fig. 8), identical to the average duration of the 1992–93 events. The longest wave event (12.7 days) occurred during the winter of 1997–98, another El Nino year. Mean event duration is similar in the 1980's and the 1990's; however, the variability in event duration is significantly larger in the 1980's. The same is true of peak near-bed wave orbital velocities during transport events in the 1980's and 1990's.

Elapsed time between transport events is important because it affects the degree of biogenic mixing or other post-depositional bed modification (e.g., consolidation) that can occur before the bed is remobilized. Non-transport intervals at a depth of 60 m ranged from <1day to >10 months, with a mean of 8 days during the winter months of 1982–99. Over the entire wave buoy record, only 3 wave events at 60 m occurred during the months of June through August. Thus during most years, the bed at water depths of 60 or more is free of wave disturbance for at least 3 months during the summer.

5. Calculations of longer-term sediment transport on the Palos Verdes shelf

A shelf sediment transport model can be used to estimate sediment transport during the resuspension events identified in the wave buoy record. In particular, estimates of the volume of sediment in suspension and of suspended sediment fluxes are useful indicators of the depth of bed reworking and the dispersal of the fine-grained sediment in the effluent-affected deposit on the Palos Verdes shelf. To determine these quantities, vertical profiles of suspended sediment concentration and

current velocity in the bottom boundary layer are required. GEOPROBE and current-meter-mooring measurements are useful for constraining such distributions, but a direct extrapolation of measured concentrations yields estimates of the volume of sediment in suspension that are too small owing to the lack of measurements close to the bed, particularly in the wave boundary layer. Numerical sediment transport models provide a means of estimating full bottom- boundary-layer concentration and velocity profiles, including effects of waves and currents. These models also permit the record of suspended sediment concentration to be extended beyond the one winter for which we have direct observations, as described below.

The sediment transport model used in these calculations is the model originally proposed for the continental shelf by Smith (1977) and most recently modified by Wiberg et al. (1994) and Harris and Wiberg (1997). This one-dimensional (vertical) model computes sediment resuspension and flux by combined wave-current shear stresses. The model accounts for moveable bed roughness, near-bed stratification, and grading of the bed resulting from preferential resuspension of finer fractions in the active layer of the bed during resuspension events. The volume of each size fraction in suspension is limited to the volume available in the surface active layer of the bed. Depth of the active layer increases with bed shear stress. The specific formulation for the active layer used in these calculations is the same as that used by Harris and Wiberg (1997) and Wiberg (in press) for mid-shelf sites in northern California.

5.1. *Specification of wave, current and bed conditions*

Shelf sediment transport models require near-bed wave and current conditions and bed sediment characteristics as input. While a long time series of near-bed wave conditions can be obtained from the buoy record, measurements of bottom-boundary-layer currents on the Palos Verdes shelf are available only for the period of the current-meter mooring deployment in 1992–93. The lack of simultaneous measurements of currents spanning the 17-years of recorded wave conditions introduces considerable uncertainty into suspended-sediment flux estimates made for specific resuspension events. However, because there is little correlation between waves and bottom-boundary-layer currents, and because mean currents are persistently directed to the northwest, calculations of mean suspended fluxes should be reasonable. The depth of bed reworking and the volume of sediment in suspension are generally more sensitive to wave conditions during a transport event than to currents. Therefore, we can obtain reasonable estimates of both using measured wave conditions and a statistically representative time series of currents as input to the model (Harris and Wiberg, 1997).

A year-long time series of near-bottom currents at 60 m was used to specify input currents for each event, as described below. Direct measurements of currents at 60 m were not made during the fall or part of the spring (Table 2). Therefore, bottom-boundary-layer currents measured at four sites on the Palos Verdes margin in 1992–93 (Noble et al., 2002) were used to construct a 10.5-month, continuous, synthetic time series of near-bottom (6 mab) currents for the shelf. A modified empirical orthogonal function (EOF) analysis (Noble et al., 2002) was used to create a representative record of near-bottom alongshelf currents 6 mab for the period from May 1992–March 1993. Over 70% of the variability in alongshelf currents measured 6 mab was accounted for by the primary EOF. The amplitude and temporal structure of the synthetic time series of along-shelf flow 6 mab agrees well with the measurements at Site B (correlation coefficient of 0.85). A similar EOF analysis could not be used to construct a synthetic time series of cross-shelf flow because the cross-shelf currents measured at the 4 mooring sites had no common spatial or temporal structure. Instead, a continuous record of cross-shelf velocity in the bottom boundary layer (6 mab) was created from a scaled average of the individual current records. The mean and standard deviation of the resulting time series were adjusted to match the average mean and standard deviation of the entire data set.

Each of the 172 wave events identified in the record from NDBC Buoy 46025 was assigned

currents from the synthetic time series that occurred on the same days of the year as that wave event. This preserved any seasonal structure in the currents that accompanied the wave events. A few wave events occurred during the 1.5-month gap during spring in the synthetic current record. Currents from the month prior to or following these wave events, whichever was closer to the time of the events, were used in these cases. Because the timing of wave events is random, this procedure results in a random assignment of currents to each event. This is reasonable because of the lack of correlation between near-bed wave orbital velocity and bottom-boundary-layer currents on the Palos Verdes shelf (see above).

The bed sediment size distribution measured at Site B (Drake et al., 2002) was assumed to describe the bed prior to each resuspension event; values of critical shear stress and settling velocity for each of the 6 size fractions are given in Wiberg and Harris (2002). Assuming a constant initial bed distribution presumes that any grading or other modification to the bed that takes place during one resuspension event is mixed away prior to the next. Bioturbation is the primary mixing process operating near the surface of the effluent-affected deposit on the Palos Verdes shelf. Measurements of biodiffusion at Site B yielded an average mixing intensity of $23\,cm^2\,yr^{-1}$ (Wheatcroft and Martin, 1996), sufficient to remix the upper few centimeters of the bed on a time scale of a week or so (Harris and Wiberg, 1997). The average time interval between events was 8 days during the winter and longer during the rest of the year. Thus it is reasonable to expect that the bed was typically remixed during the time interval between resuspension events.

5.2. Model results

Comparison of calculated light attenuation with values measured by the GEOPROBE during the winter of 1992–93 provides a test of model performance. Model-derived attenuation is found by applying the size-dependent transmissometer calibration (Fig. 3a) to calculated suspended sediment concentrations (see Wiberg et al., 1994). Attenuation calculated for the 1992–93 winter wave and current conditions is consistent with measured attenuation during deployments B2 and B3 (Fig. 9). The correlation between low-pass filtered calculated and measured attenuation during these deployments is 0.91 (0.3 mab) and 0.85 (1.0 mab) during deployment B2 and 0.85 (0.3 mab) and 0.76 (1.0 mab) during deployment B3. The correlation between calculated and measured attenuation is lower (0.3–0.4) during the first deployment (B1) because elevated attenuation during that early winter period was not well correlated with either waves or currents. The agreement between measured attenuation and calculated concentration at times when pump samples were collected ($r^2 = 0.72$; Fig. 10a) is similar to that between measured attenuation and concentrations observed in pump samples ($r^2 = 0.80$, Fig. 3b) during deployments B2 and B3.

The timing and magnitude of calculated and measured attenuation for the 3 wave-driven resuspension events that occurred during the GEOPROBE deployments (events 4, 5 and 6, Table 3) agree well overall (Fig. 9a and b). The pump samples that were collected during these events are also generally consistent with calculated concentrations (Fig. 9c). Mean values of calculated attenuation 0.3 mab are 0–28% lower than mean measured values for the 3 events, while mean calculated attenuation 1.0 mab is 0–42% higher than observed (Table 3). As a result, the near-bed gradient in calculated mean attenuation is lower than measured. Attenuation and concentration profiles tend to be more uniform as sediment size decreases because of lower settling velocities and stronger attenuation response (Fig. 3a). This suggests that the model may be overestimating the relative amount of the finest size fractions in suspension. Calculated mean suspended particle size for these events (22 μm at 0.3 mab and 18 μm at 1.0 mab) generally agree with the measured size of sediment in pump samples. However, the calculated size distributions 0.3 mab tend to underestimate the $>45\,\mu m$ fraction.

The model underestimates measured attenuation for a period of several days to a week after events 5 and 6 (Fig. 9a and b); the time between events 4 and 5 is too short to see a similar effect

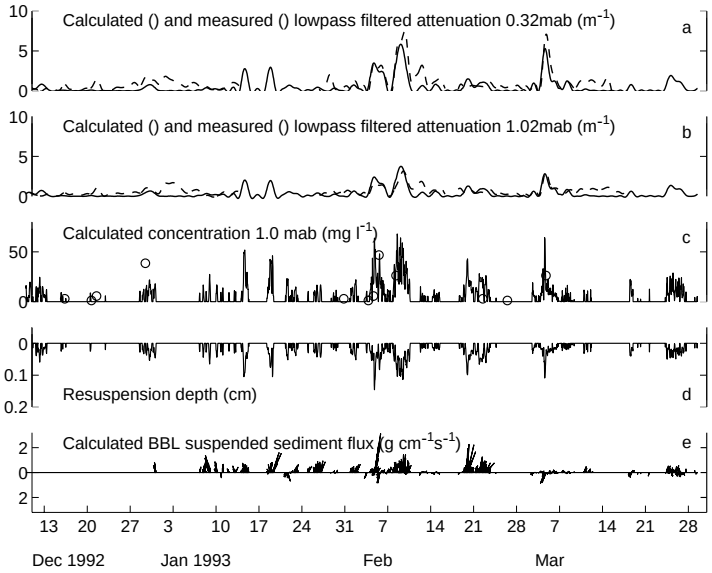

Fig. 9. Comparison of measured and calculated low-pass filtered attenuation (a) 0.3 mab and (b) 1.0 mab and calculated values of (c) concentration 1.0 mab, (d) resuspension depth and (e) suspended sediment flux in the bottom boundary layer at Site B during the winter of 1992–93. The circles in (c) indicate concentrations measured in pump samples collected 1 mab.

after event 4. One explanation for the discrepancy is that recent deposits of fine-grained sediment have a higher porosity and lower critical shear stress than sediment that has had up to a week to consolidate (e.g., Toorman, 1998). As a result, relatively small waves or strong tidal currents immediately following a sediment transport event have a greater-than-usual potential for resuspending bed surface sediment. In addition to the wave-driven resuspension events in 1992–93 discussed above, the model indicates one period of elevated suspended sediment concentration and flux during a period of high, sustained subtidal currents at the beginning of deployment B3 (mid February; Fig. 9c). Measured and calculated attenuation during this time are in reasonably good agreement, but the concentration in the 1 mab pump sample (indicated by the circle on 22 February in Fig. 9c) is lower than the average calculated concentration. The pump sampling interval (<1 min) might have occurred at a time when concentration was low or the model might be overestimating suspended concentrations, particularly of coarser particles with higher concentration-attenuation ratios (Fig. 3a), during this current-driven event.

The volume of sediment in suspension and the suspended sediment flux can be found by integrating calculated profiles of concentration and of the product of velocity and concentration, respectively, over the height of the bottom boundary layer. Maximum calculated suspended-sediment volume at Site B during the winter of 1992–93 was $0.035\,\mathrm{cm^3\,cm^{-2}}$ (4 February). Suspended-sediment volume divided by bed porosity (0.24 for the upper 2 cm of the bed at Site B; Fig. 10b of Lee et al., 2002) gives the thickness of the bed layer required to supply the volume of sediment in suspension. We refer to the maximum thickness of this bed layer during a resuspension event as the resuspension depth. The average resuspension depth was 0.11 cm during the 6 wave events in 1992–93 for which we know both near-bed waves and currents; the maximum calculated resuspension depth was 0.15 cm (Table 3). The direction of suspended sediment flux for each event is given by the mean current direction (Table 3). Net suspended sediment flux in 1992–93 was toward the northwest for all but one of the modeled resuspension events; net flux was southeastward during event 6 (Table 3). Maximum calculated flux was $3.1\,\mathrm{g\,cm^{-1}\,s^{-1}}$ (event

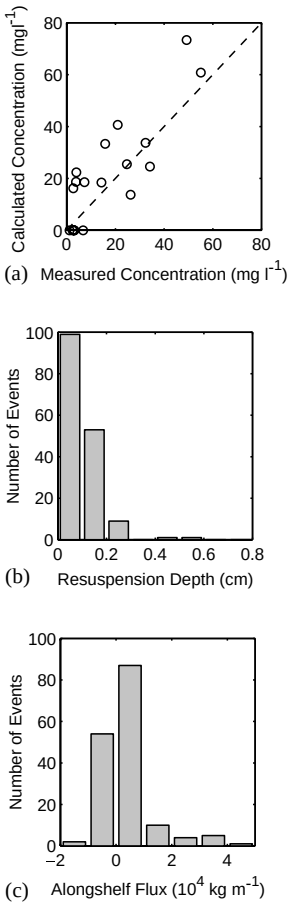

Fig. 10. (a) Calculated concentration vs. concentration measured in GEOPROBE pump samples collected at Site B; $r^2 = 0.72$. (b) Distribution of calculated resuspension depth during transport events at Site B identified in the wave buoy record from 1982–99. Resuspension depth is defined as the peak volume of sediment in suspension during a transport event divided by bed porosity (0.24); mean resuspension depth is 0.1 cm. (c) Distribution of total alongshelf transport ($kg\,m^{-1}\,event^{-1}$) calculated for wave-driven resuspension events at Site B from 1982–99; positive values indicate poleward (northwest) alongshelf transport. Total alongshelf transport averages $3600\,kg\,m^{-1}\,event^{-1}$ and is directed northwest along the shelf.

4; Fig. 9e). Average net alongshelf flux per event for the 5 modeled events with poleward transport is $120\,kg\,m^{-1}\,h^{-1}$; net across-shelf flux is an average of 10 times smaller than along-shelf flux (Table 3). Net alongshelf flux was much smaller ($30\,kg\,m^{-1}\,h^{-1}$) for the one equatorward transport event.

The pattern of alongshelf sediment transport calculated for the 172 wave events identified at Site B in the NDBC Buoy 46025 record is similar to that observed during the winter of 1992–93, though the average transport rate per event is higher than it was in winter 1992–93. Mean resuspension depth calculated for all events in the buoy record is 0.10 cm (Fig. 10b). The largest resuspension depth, 0.55 cm, is associated with the January 1988 event. Net alongshelf sediment flux is poleward for two-thirds of the 172 resuspension events (Fig. 10c), with an average rate of $140\,kg\,m^{-1}\,h^{-1}$. The net alongshelf flux for the remaining (equatorward) events is smaller, averaging $50\,kg\,m^{-1}\,h^{-1}$. Average net across-shelf flux is negligible. Total net transport per event (integrated transport over each event) averaged $6400\,kg\,m^{-1}$ and $1900\,kg\,m^{-1}$ during poleward and equatorward transport events, respectively (Fig. 10c). These values are about 50% higher than corresponding rates for the winter of 1992–93. Summing over all wave-driven transport events at Site B from 1982–1999, 87% of calculated suspended sediment flux is alongshelf to the northwest.

6. Conclusions

GEOPROBE and current-meter mooring data from Site B during the winter of 1992–93, together with analyses of bed samples from the site, provide an exceptional set of observations of bottom-boundary-layer flow and sediment transport on the Palos Verdes shelf. Based on these observations, it is clear that sediment at depths near 60 m in the effluent-affected deposit is frequently resuspended during winter storms. Wave-driven resuspension events at Site B are observed when peak $u_{bs} \geqslant 14\,cm\,s^{-1}$. Seven transport events were identified in the record of bottom wave conditions at Site B during the winter of 1992–93. Net suspended sediment flux during these events was directed alongshelf, toward the northwest. This is consistent with the footprint of the effluent-affected sediment layer on the Palos Verdes shelf, which also extends to the northwest from the Whites Point outfalls (see Lee et al., 2002).

Terrigenous (mineral) sediment resuspended from the bed was the predominant material in suspension during periods of relatively high concentration ($>10\,mg\,l^{-1}$), while biogenic detritus dominated when concentrations were low.

The record of surface waves during 1982–99 from NDBC Buoy 46025 suggests that the winter of 1992–93 was a moderate year in terms of the frequency and intensity of wave-driven transport events. Good agreement between near-bed wave orbital velocities calculated from buoy spectral data and from GEOPROBE velocity measurements confirms that the wave buoy data can be used to extend characterizations of sediment transport on the shelf in space and time. Wave conditions on the Palos Verdes shelf are sufficient to resuspend sediment an average of 10 days per year at a depth of 60 m. At a depth of 90 m, wave-driven resuspension is estimated to occur only about 1.5 days per year. The deepest location at which the resuspension threshold was exceeded during 1982–99 is 170 m, on the upper slope.

A shelf sediment transport model that has been used to investigate transport at two mid-shelf sites in northern California (Russian and Eel River shelves) performs well at Site B with no adjustment of coefficients. Calculated attenuation, low-pass filtered to remove the short-term variability associated with tidal currents, is well correlated with measured attenuation ($\geqslant 0.8$) during the period of observation from late January to mid-March, 1993. The correlation is poorer in mid-December to early January when waves are relatively low and variations in turbidity appear not to have been controlled by the prevailing waves and currents. The total amount of suspended-sediment transport at Site B, averaged over all resuspension events during 1982–99, is calculated to be $3600\,kg\,m^{-1}\,event^{-1}$ and is directed alongshelf to the northwest.

Resuspension alone does not appear to mobilize more than the uppermost centimeter of the bed at Site B. Net erosion due to a divergence in suspended sediment flux along or across the shelf (Sherwood et al., 2002; Harris and Wiberg, 2001) would be necessary to rework a deeper layer of the bed. Somewhat higher alongshelf mean currents at Site D compared to Site B suggest this possibility (Table 2). However, mean alongshelf current at Site D was 30% smaller than at Site B, and oriented in the opposite direction, during the wave-driven transport events in the winter of 1992–93, suggestive of flux convergence and net deposition between the two sites during that winter. A longer period of current observations or a coupled shelf-circulation sediment-transport model would be necessary to deduce any long-term trend of along-shelf net deposition or erosion between Sites B and D due to variations in alongshelf currents. Changes in bed sediment characteristics can also lead to flux divergence. The importance of this contribution to net erosion or deposition on the Palos Verdes shelf is considered in Sherwood et al. (2002).

Acknowledgements

Financial support for this study was provided by the National Oceanic and Atmospheric Administration and by the US Geological Survey. We gratefully acknowledge George Tate, Joanne Thede-Ferriera, Rick Viall and Dave Cacchione for their indispensable help with the complex preparations, deployments and recoveries of the GEOPROBE tripods and with the subsequent analysis of the data. Bill Strahle and Marinna Martini handled the design and deployment/recovery of the highly successful current meter moorings in their usual professional manner. Kaye Kinoshita provided invaluable support with both the field operations and data analysis. The capable seamanship, experience and onshore support of the staff of the USC Marine Facility were key to the success of our research. The paper benefited from the helpful review comments of Brad Butman, Carl Friedrichs and Nathan Hawley.

References

Borgman, L.E., Resio, D.T., 1982. Extremal statistics in wave climatology. In: Osborne, A., Rizzoli, P.M. (Eds.), Topics in Ocean Physics. Italian Physical Society, Bologna, Italy, pp. 439–471.

Cacchione, D.A., Drake, D.E., 1990. Shelf sediment transport: an overview with applications to the northern California

continental shelf. In: LeMehaute, B., Hanes, D. (Eds.), The Sea, Vol. 9. Wiley, New York, pp. 729–773.

Drake, D.E., Cacchione, D.A., 1985. Seasonal variation in sediment transport on the Russian River shelf, California. Continental Shelf Research 4, 495–514.

Drake, D.E., Cacchione, D.A., 1992. Wave-current interaction in the bottom boundary layer during storm and non-storm conditions. Continental Shelf Research 12, 1331–1352.

Drake, D.E., Eganhouse, R.P., McArthur, W., 2002. Physical and chemical effects of grain aggregates on the Palos Verdes margin, southern California. Continental Shelf Research 22, 967–986.

Harris, C.K., Wiberg, P.L., 1997. Approaches to quantifying long-term continental shelf sediment transport with an example from the northern California STRESS mid-shelf site. Continental Shelf Research 17, 1389–1418.

Harris, C.K., Wiberg, P.L., 2001. A two-dimensional, time-dependent model of suspended sediment transport and bed reworking for continental shelves. Computers and Geosciences 27, 675–690.

Lee, H.J., Sherwood, C.R., Drake, D.E., Edwards, B.D., Wong, F., Hamer, M., 2002. Spatial and temporal distribution of contaminated, effluent-affected sediment on the Palos Verdes margin, southern California. Continental Shelf Research 22, 859–880.

Madsen, O.S., Wright, L.D., Boon, J.D., Chisholm, T.A., 1993. Wind stress, bed roughness and sediment suspension on the inner shelf during an extreme storm event. Continental Shelf Research 13, 1303–1324.

National Oceanographic Data Center, 1998. NOAA Marine Environmental Buoy Data Webdisc CD-ROM set (7 disks). Silver Springs, MD: National Oceanographic Data Center.

National Oceanographic Data Center, 2000. NOAA Marine Environmental Buoy Database (NODC File 291), www.nodc.noaa.gov/BUOY/buoy.html.

Noble, M.A., Ryan, H.F., Wiberg, P.L., 2002. The dynamics of subtidal poleward flows over a narrow continental shelf, Palos Verdes, CA. Continental Shelf Research 22, 923–944.

Ogston, A.S., Sternberg, R.W., 1999. Sediment-transport events on the northern California continental shelf. Marine Geology 154, 69–82.

Sherwood, C.R., Butman, B., Cacchione, D.A., Drake, D.E., Gross, T.F., Sternberg, R.W., Wiberg, P.L., Williams III, A.J., 1994. Sediment transport events of the northern California continental shelf during the 1990–1991 STRESS experiments. Continental Shelf Research 14, 1063–1099.

Sherwood, C.R, Drake, D.E., Wiberg, P.L., Wheatcroft, R.A., 2002. Prediction of the fate of *p,p′*-DDE in sediment on the Palos Verdes shelf, California, USA. Continental Shelf Research 22, 1025–1058.

Smith, J.D., 1977. Modeling of sediment transport on continental shelves. In: Goldberg, E.D., McCave, I.N., Obrien, J.J., Steele, J.H. (Eds.), The Sea, Vol. 6, Marine Modeling. Wiley, New York, pp. 539–577.

Stull, J.K., Haydock, C.I., Smith, R.W., Montage, D.E., 1986. Long-term changes in the benthic community on the coastal shelf of Palos Verdes, southern California. Marine Biology 91, 539–551.

Stull, J.K., Baird, R., Heesen, T., 1988. Relationship between declining discharges of municipal wastewater contaminants and marine sediment core profiles. In: Wolfe, D.A., O'Conner, T.P., Krieger, R.E. (Eds.), Oceanic Processes in Marine Pollution 5. R.E. Krieger Publishing Co., Malabar, FL, pp. 23–32.

Toorman, E.A., 1998. Sedimentation and self-weight consolidation: constitutive equations and numerical modeling. Geotechnique 49, 709–726.

Wheatcroft, R.A., Martin, W.R., 1996. Spatial variation in short-term (^{234}Th) sediment bioturbation intensity along an organic-carbon gradient. Journal of Marine Research 54, 763–792.

Wiberg, P.L., 1995. A theoretical investigation of boundary layer flow and bottom shear stress for smooth, transitional, and rough flow under waves. Journal of Geophysical Research 100, 22667–22679.

Wiberg, P.L., 2000. A perfect storm: the formation and potential for preservation of storm beds on the continental shelf. Oceanography 13, 93–99.

Wiberg, P.L., Harris, C.K., 2002. Desorption of *p,p′*-DDE from sediment during resuspension events on the Palos Verdes shelf, California: a modeling approach. Continental Shelf Research 22, 1005–1023.

Wiberg, P.L., Drake, D.E., Cacchione, D.A., 1994. Sediment resuspension and bed armoring during high bottom stress events on the northern California inner continental shelf: Measurements and predictions. Continental Shelf Research 14, 1191–1220.